Purdue University
Purdue e-Pubs

International Refrigeration and Air Conditioning Conference

School of Mechanical Engineering

2008

# An Experimental Study on Void Fraction of CO2 Flow Boiling in a Horizontal Micro-fin Tube

Chieko Kondou
*Hitachi Appliances*

Ken Kuwahara
*Kyushu University*

Shigeru Koyama
*Kyushu University*

# An Experimental Study on Void Fraction of $CO_2$ Flow Boiling in a Horizontal Micro-fin Tube

Chieko KONDOU[1]*, Ken KUWAHARA [2] and Shigeru KOYAMA[2]

[1] Technology Development Department, Shimizu Air Conditioning Works, Hitachi Appliances, Inc.
390 Muramatsu, Shimizu, Shizuoka, Japan
Phone: +81-543-35-9903, Fax: +81-543-36-0776, E-mail: chieko.kondo.mz@hitachi.com

[2] Faculty of Engineering Sciences, Kyushu University
6-1 Kasugakoen, Kasuga, Fukuoka, Japan
Phone:+81-92-583-7831, Fax: +81-92-583-7833

## ABSTRACT

This paper deals with an experimental investigation on the void fraction of $CO_2$ in a horizontal micro-fin tube. The void fraction was measured by the quick closing valve method under boiling conditions. The experimental data were obtained in the range of refrigerant mass flux from 200 to 455 kg $m^{-2}$ $s^{-1}$ and the pressure range from 3.5 to 5.0 MPa, and were compared with two literature data. One is the empirical correlation by Butterworth and another is the correlation with equal velocity head model by Smith. The slip ratio, obtained from experimental data of void fraction, increased drastically in vapor quality of over 0.9. The present data agree with Butterworth's correlation in vapor quality ranging from 0.03 to 0.99. However, this correlation has not taken into account an effect of refrigerant mass flux. Consequently, as a trial, a widely applicable empirical correlation considering the effect of mass flux is proposed to predict the void fraction of refrigerants $CO_2$, R 22, R 410A, R 134a and R 12.

## 1. INTRODUCTION

Micro-fin tubes make it possible for performance increase and size and cost reduction of cross-finned heat exchangers. Recently, such tubes have been used in air conditioning and refrigerating appliances. Therefore, a lot of investigations on heat transfer and pressure drop characteristics of many kinds of refrigerants in micro-fin tubes have been carried out. However, the reports on the void fraction seem insufficient, though the void fraction is important for the estimation of heat transfer and pressure drop inside micro-fin tubes. The void fraction is also one of the important parameters to predict the amount of refrigerant in heat exchangers. Yashar *et al*. (2001) examined the void fraction of R 134a and R 410A in horizontal micro-fin tubes and verified the difference between smooth and micro-fin tubes. Koyama *et al*. (2004) experimentally investigated the void fraction of R 134a in horizontal micro-fin tubes and discussed the effects of saturation pressure.

This study provides the experimental results of the void fraction of $CO_2$ in a horizontal copper micro-fin tube under boiling conditions by means of the quick closing valve method. Carbon dioxide, as the working fluid, makes it possible to verify the effect of density ratio between vapor and liquid on the void fraction at a higher reduced pressure than other refrigerants. In addition, the slip ratios are obtained from the experimental data of void fraction and compared with previous studies. As a trial, an empirical correlation between the slip ratio and the vapor quality has been proposed.

## 2. EXPEPERIMENTAL TECHNIQUE

### 2.1 Test loop and sampling section

Figure 1 shows a schematic diagram of the experimental refrigeration cycle. This cycle mainly consists of a compressor (1), an oil separator (2), four cooling water jackets (3), a receiver tank (4), a mass flow meter (5), an

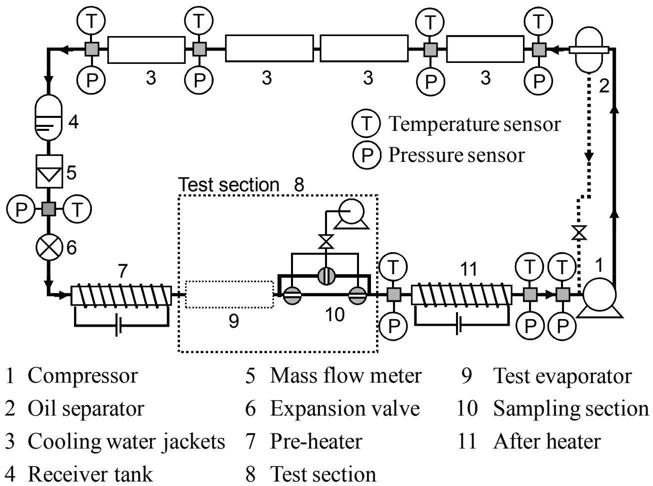


Figure 1: Schematic diagram of experimental refrigeration cycle

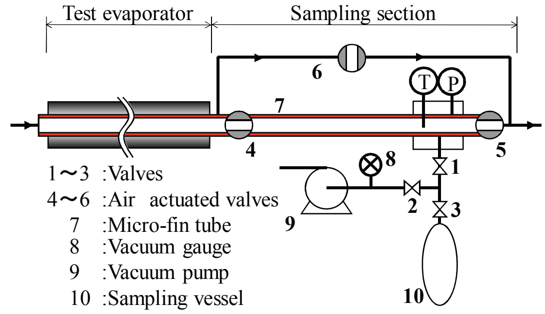


Figure 2: Schematic view of test section

Table 1: Specification of sampling section

| | |
|---|---|
| Length of sampling zone | 400.0 mm |
| Sampling volume ($V_{samp}$) | 10183 mm$^3$ |
| Residual volume ($V_{rest}$) | 14167 mm$^3$ |
| Dead space ($V_{dead}$) | 417 mm$^3$ |
| Diameter of valve orifice | 4.8 mm |

expansion valve (6), a pre-heater (7), a test section (8) and an after-heater (11). The test section was composed of two parts, the test evaporator (9) and the sampling section (10). The vapor quality was precisely controlled by the water flow rate regulation in this test evaporator. The mean void fraction in this sampling section, which was next to the test evaporator, was measured by the quick closing valve method. Eight mixing chambers, for measuring refrigerant bulk temperature and pressure, were located next to each main element in this cycle. The calibration accuracies of the temperature sensors were 0.05K, and the pressure transducers were accurate to 4 kPa. The refrigerant mass flow rate was measured with a Coriolis-type mass flow meter (5), located next to the receiver tank, within 0.28 kg h$^{-1}$ accuracy. It should be noted that sampling section was insulated. Furthermore, most of above two parts in the test section, with the exception of the orifice in the ball valve, consisted of horizontal copper micro-fin tubes.

Figure 2 shows a schematic view of the test section, which is composed of test evaporator and sampling section. The procedure to measure the void fraction is described as follows:

(1) Preliminarily, valves (1) and (6) are closed, while valves (2), (3), (4) and (5) are opened. Valves (4), (5) and (6) are actuated by compressed air.
(2) Inside of vessel is evacuated by vacuum pump (9), and valve (2) is closed to keep this condition. Here, the arrangement for measuring the void fraction is competed.
(3) Valves (4) and (5) are closed instantaneously; valve (6) is opened simultaneously.
(4) Valve (1) is open to take sampled refrigerant into the vessel. Next, valve (3) is closed, and the sampling vessel is detached from the sampling section. Finally, the sampling vessel is weighed using an electronic balance of 1 mg in minimum measuring mass.

The specification of sampling section is listed in Table 1 for reference.

## 2.2 Test tube and test condition

Table 2 lists the dimensions of the test tube, and Fig. 3 is a schematic diagram of the dimensions listed in Table 2. The “equivalent I.D.” is the inner diameter of an equivalent smooth tube, which has the same cross sectional area. The “area enlargement ratio” is the ratio of the extended heat transfer area inside the micro-fin tube to the heat transfer area inside an equivalent smooth tube. Table 3 lists the test conditions. A mass flux ranged from 200 to 455 kg m$^{-2}$ s$^{-1}$, and heat flux ranged from 10 to 20 kW m$^{-2}$. The experiment was conducted at saturated pressure between 3.5 and 5.0 MPa, in other words, equal to the reduced pressure between 0.47 to 0.68.

## 2.3 Data reduction method

Figure 4 shows the data reduction method of mean vapor quality at the sampling section. The bulk temperature $T_{MC}$ and pressure $P_{MC}$ of superheated vapor are measured in the mixing chamber next to the after heater. In parallel, the pressure differences $\Delta P_{AH}$ and $\Delta P_{void}$ are measured with a differential pressure transducer. The heat transfer rate at the after heater $Q_{AH}$ and the refrigerant mass flow rate $W_r$ are also measured. The specific enthalpy $h_{MC}$ in the

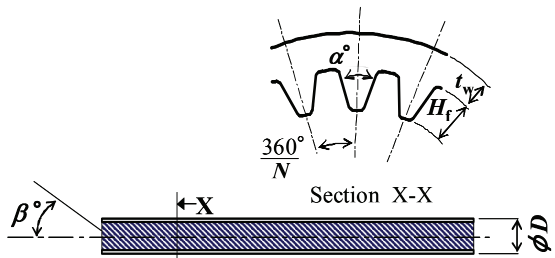


Figure 3: Dimension of test micro-fin tube

Table 2: Dimension of test micro-fin tube

| | | |
|---|---|---|
| O.D. | $D$ | 7.00 mm |
| Equivalent I. D. | $d_i$ | 5.67 mm |
| Thickness | $t_w$ | 0.60 mm |
| Fin height | $H_f$ | 0.23 mm |
| Number of fins | $N$ | 50 - |
| Apex angle | $\alpha$ | 30 ° |
| Helix angle | $\beta$ | 15 ° |
| Area increase ratio | $\eta$ | 184 % |

Table 3: Test condition

| № | Pressure | Mass flux | Heat flux |
|---|---|---|---|
| I | $P$=3.5 MPa | $G_r$=200 kg m$^{-2}$s$^{-1}$ | $q$=20 kW m$^{-2}$ |
| II | | | $q$=10 kW m$^{-2}$ |
| III | | $G_r$= 350 kg m$^{-2}$s$^{-1}$ | $q$=20 kW m$^{-2}$ |
| IV | | | $q$=10 kW m$^{-2}$ |
| V | $P$=5.0 MPa | $G_r$=200 kg m$^{-2}$s$^{-1}$ | $q$=20 kW m$^{-2}$ |
| VI | | | $q$=10 kW m$^{-2}$ |
| VII | | $G_r$= 350 kg m$^{-2}$s$^{-1}$ | $q$=20 kW m$^{-2}$ |
| VIII | | | $q$=10 kW m$^{-2}$ |
| IX | | $G_r$=455 kg m$^{-2}$s$^{-1}$ | $q$=20 kW m$^{-2}$ |

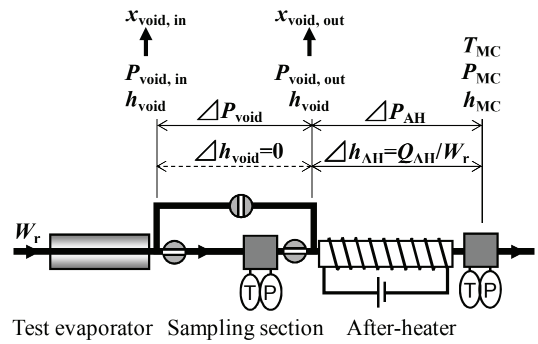


Figure 4: Procedure of data reduction

mixing chamber is calculated from temperature $T_{MC}$ and pressure $P_{MC}$. The specific enthalpy $h_{void}$ in the mixing chamber is obtained as,

$$h_{void,in} = h_{void,out} = h_{MC} - Q_{AH}/W_r \tag{1}$$

Next, the entrance vapor quality $x_{viod,in}$ is calculated from specific enthalpy $h_{void}$ and pressure $P_{void,in}$, while the exit vapor quality $x_{void,out}$ is calculated from specific enthalpy $h_{void}$ and pressure $P_{void,out}$. The mean vapor quality $x_{void}$ is defined as the arithmetic mean of the entrance and exit.

The refrigerant mass $m_{samp}$, which was trapped in the sampling tube, is estimated as follows,

$$m_{samp} = m_{ves} + \rho_{SG} V_{rest} - \rho_G V_{dead} \tag{3}$$

where $m_{ves}$ is the mass of the refrigerant mass in the sampling vessel, $\rho_{SG}V_{rest}$ is the remaining refrigerant mass from the sampling tube to valve (3) detached with sampling vessel. The density $\rho_{SG}$ is the vapor density after closing valve (3) for sealing sampled refrigerant in the vessel. The third term in Eq. (3) expresses the refrigerant mass in dead space, a stagnant space like the insert hole for the thermo sensor. The volume of dead space accounts for 4% of the sampling volume.

Finally, the void fraction is obtained from the following equation,

$$\xi = \frac{V_G}{V_{samp}} = \frac{\rho_L V_{samp} - m_{samp}}{\left(\rho_L - \rho_G\right) V_{samp}} \tag{2}$$

where $\rho_L$ and $\rho_G$ are the densities of liquid and vapor, respectively, inside the sampling tube before trapping the refrigerant inside it.

## 3. RESULTS AND DISCUSSION

### 3.1 Experimental results on void fraction

Figure 5 (a) shows the effect of heat flux on the relation between void fraction and vapor quality at 5.0 MPa.

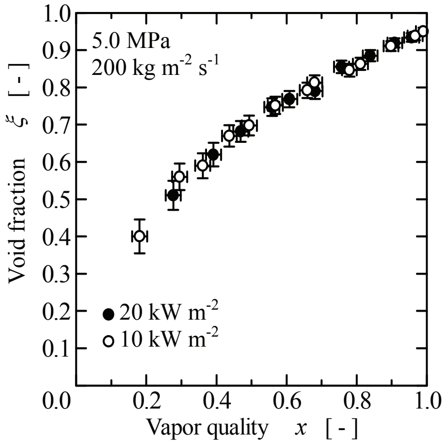


(a) Effect of heat flux

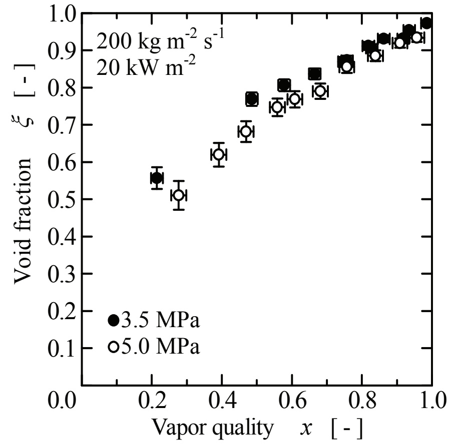


(b) Effect of saturation pressure

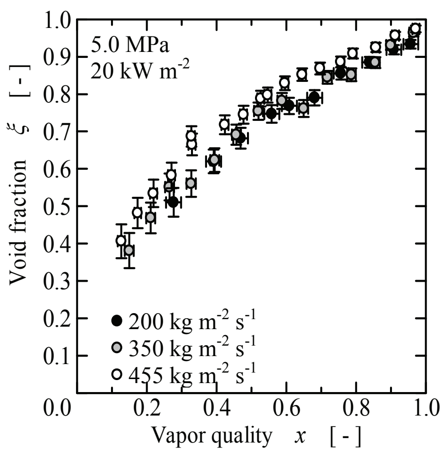


(c) Effect of mass flux

Figure 5: Experimental results of void fraction against vapor quality

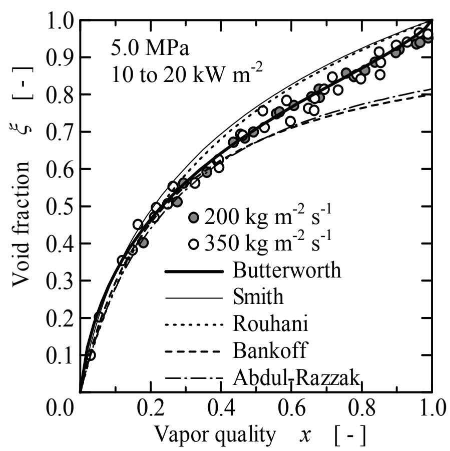


Figure 6: Previous correlations with present experimental data

Figure 5 (b) shows the effect of saturation pressure on the relation between void fraction and vapor quality. Figure 5 (c) shows the effect of refrigerant mass flux on the relation between void fraction and vapor quality. The error bars on these figures correspond to 95% confidence level. The void fraction against vapor quality is unchanged against the heat flux. A similar tendency has been described by Yashar *et al*. (2001). On the other hand, the void fraction decreases due to the pressure increase. Koyama *et al*. (2004) have already confirmed that the increase of density ratio of vapor to liquid, along with the reduced pressure increase, decreases void fraction. The present data of Fig. 5 (b) agree with those confirmations. In terms of refrigerant mass flux, the difference between the void fraction at 200 and 350 kg m$^{-2}$ s$^{-1}$ is not clear. However, the results of void fraction at 455 kg m$^{-2}$ s$^{-1}$ are slightly higher than those at 200 and 350 kg m$^{-2}$ s$^{-1}$. This slight effect of refrigerant mass flux is also discernible in the reports by Wojtan *et al*. (2004), Yashar *et al*. (2001), and Koyama *et al*. (2004).

### 3.2 Comparison with previous correlations

Many correlations of void fraction in smooth tubes have been proposed. However, no correlation seems to be proposed for micro-fin tubes. As a trial, the present experimental results are compared with some of correlations for smooth tubes. Figure 6 shows a comparison with the present experimental results and correlations from Butterworth (1975), Smith (1971), Rohani *et al*. (1970), Bankoff (1960), and Abdul-Razzak *et al*. (1995). Butterworth's correlation overlapped the most with the present experimental data.

Figure 7 (a) shows a slip ratio based on the refrigerant mean velocities of vapor and liquid phases as shown in Fig. 7 (b). These data of mean velocities and the slip ratio are obtained from the following equations,

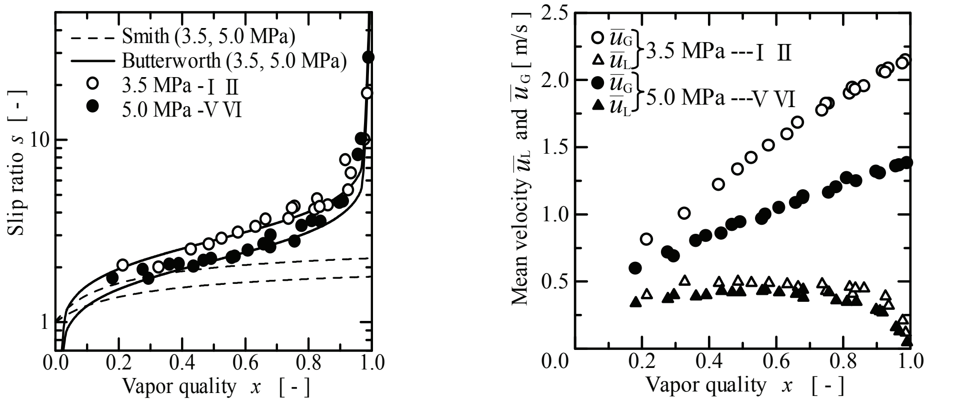


(a) Slip ratio (b) Mean velocity of vapor and liquid phase

Figure 7: Slip ratio between liquid and vapor phase refrigerant

$$\bar{u}_G = \left( \frac{xG_r}{\rho_G} \right) \Big/ \xi \tag{4}$$

$$\bar{u}_L = \left[ \frac{(1-x)G_r}{\rho_L} \right] \Big/ (1-\xi) \tag{5}$$

$$s = \frac{\bar{u}_G}{\bar{u}_L} = \left( \frac{x}{1-x} \right) \left( \frac{\rho_L}{\rho_G} \right) \left( \frac{1-\xi}{\xi} \right) \tag{6}$$

As shown in Fig. 7(a), the experimental data of slip ratio drastically increases when vapor quality is over 0.9. The same feature of the slip ratio has been reported by Koyama *et al*. (2004). In this figure, the slip ratio predicted by correlations of Smith and Butterworth are also drawn by solid and dashed lines, respectively. Experimental data agree well with Butterworth's correlation, while Smith's correlation underestimates the slip ratio in high quality region. It is noted that the difference in the slip ratio causes only a small difference in the void fraction between Smith's and Butterworth's correlations.

As shown in Fig. 7(b), the mean velocity of vapor phase increases almost proportionally due to an increase in vapor quality. On the contrary, the mean velocity of liquid phase has a gentle peak at vapor quality of 0.5, and decreases drastically at vapor quality over 0.9. These changes of mean velocities cause the drastic increase of the slip ratio at the quality over 0.9 as shown in Fig. 7(a).

## 3.3 Modification of the correlation for void fraction against vapor quality

As a trial, Smith's model for smooth tube is modified to predict the slip ratio and the void fraction in both micro-fin and smooth tubes. At first, the effects of refrigerant properties and mass flux are evaluated from present and previous data including data for smooth tubes. Secondly, the effects of friction inside micro-fin and smooth

Table 4: Main comparative database specifications of previous experimental

| Authers | Tube | Measurement method | Refrigerant | Equivalent inner diameter $d_i$ [ mm ] | Pressure $P$ [ MPa ] | Mass flux $G_r$ [ kg m$^{-2}$ s$^{-1}$] | Desity ratio $\rho_G / \rho_L$ [ - ] |
|---|---|---|---|---|---|---|---|
| *Wojtan et al.* | Smooth | visualization | R 22 | 13.6 | 0.58 | 70 to 200 | 0.0195 |
| *Wojtan et al.* | Smooth | visualization | R 410A | 13.6 | 0.93 | 70 to 300 | 0.0311 |
| *Abdul-Razzak et al.* | Smooth | gamma densitometer | R 134a | 10.7 | 0.78 | 78 to 670 | 0.0321 |
| *Hashizume* | Smooth | quick closing valves | R 12 | 10.0 | 1.22 | 25 to 100 | 0.0575 |
| *Koyama et al.* | Micro-fin | quick closing valves | R134 a | 8.9 | 1.20 | 90 to 180 | 0.0534 |
| *Yashar et al.* | Micro-fin | quick closing valves | R 134a | 8.8 | 0.35 | 75 to 500 | 0.0134 |
| Present data | Micro-fin | quick closing valves | $CO_2$ | 5.7 | 3.5 | 200 to 350 | 0.1059 |
| Present data | Micro-fin | quick closing valves | $CO_2$ | 5.7 | 5.0 | 200 to 455 | 0.1894 |

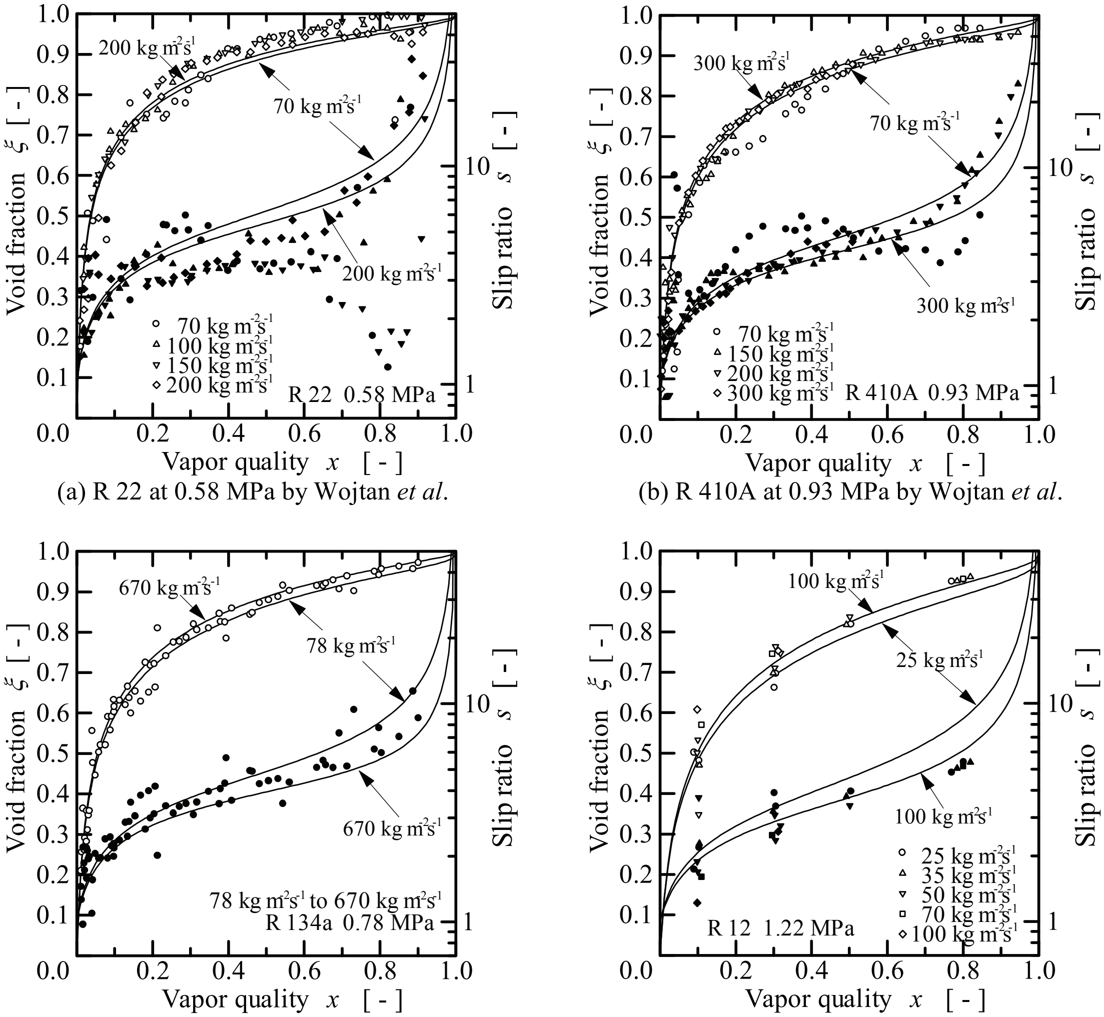


(a) R 22 at 0.58 MPa by Wojtan *et al*.

(b) R 410A at 0.93 MPa by Wojtan *et al*.

(c) R 134a at 0.78 MPa by Abdul-Razzak *et al*.

(d) R 12 at 1.22 MPa by Hashizume

Figure 8: Comparison of present correlation with previous data of smooth tubes

tubes are evaluated from present and previous data. The void fraction is given in Eq. (7).

$$\xi = \frac{x}{x + s_{\mathrm{T}}\left(1-x\right)\left(\rho_{\mathrm{G}}/\rho_{\mathrm{L}}\right)} \tag{7}$$

The slip ratio $s_{\mathrm{T}}$ is assumed as the sum of the momentum and frictional terms, and expressed by Eq. (8).

$$s_{\mathrm{T}} = s_{\mathrm{M}} + s_{\mathrm{F}} \tag{8}$$

Then, the momentum term of the slip ratio $s_{\mathrm{M}}$ is assumed to be obtained by Smith's model described as Eq. (9).

$$s_{\mathrm{M}} = e + \left(1-e\right)\left[\frac{1 + e\left(\dfrac{1-x_{\mathrm{v}}}{x_{\mathrm{v}}}\right)}{\dfrac{\rho_{\mathrm{G}}}{\rho_{\mathrm{L}}} + e\left(\dfrac{1-x_{\mathrm{v}}}{x_{\mathrm{v}}}\right)}\right]^{\frac{1}{2}} \tag{9}$$

where $e$ is the entrainment factor, the recommended value of which is 0.4, and the volume dryness fraction $x_{\mathrm{v}}$ is given in Eq. (10).

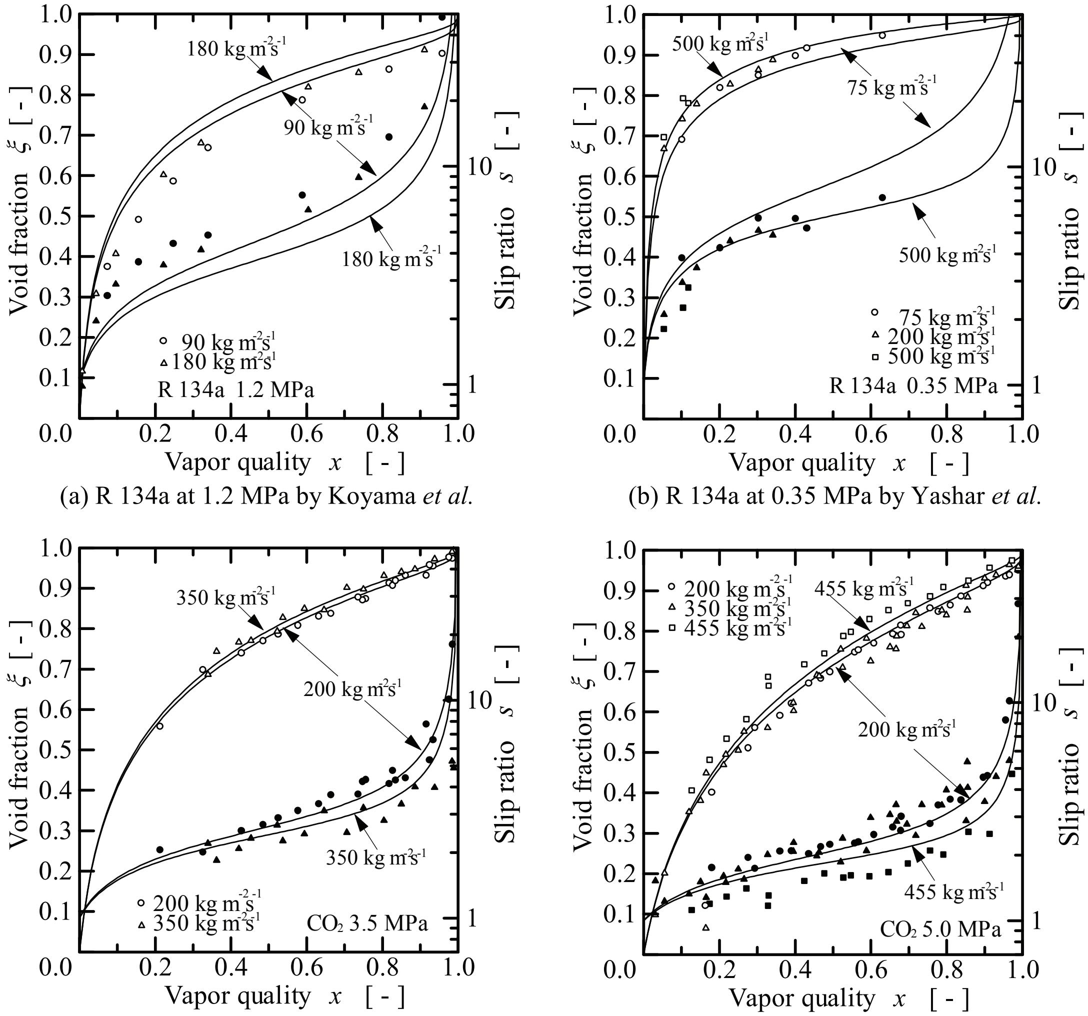


(a) R 134a at 1.2 MPa by Koyama *et al.* (b) R 134a at 0.35 MPa by Yashar *et al.*

(c) Present data $CO_2$ at 3.5MPa (d) Present data $CO_2$ at 5.0MPa

Figure 9: Comparison of present correlation with previous data of micro-fin tubes

$$x_{\mathrm{v}} = \frac{x}{x + (1-x)(\rho_{\mathrm{G}}/\rho_{\mathrm{L}})} \tag{10}$$

In the wake of Butterworth's empirical correlation, the frictional term of the slip ratio $s_{\mathrm{F}}$ is assumed to be expressed as Eq. (11).

$$s_{\mathrm{F}} = A\left(\frac{1-x}{x}\right)^{p}\left(\frac{\rho_{\mathrm{G}}}{\rho_{\mathrm{L}}}\right)^{q}\left(\frac{\mu_{\mathrm{L}}}{\mu_{\mathrm{G}}}\right)^{r}\left(\frac{G_{\mathrm{r}}}{\sqrt{g d_{\mathrm{i}} \rho_{\mathrm{G}} (\rho_{\mathrm{L}} - \rho_{\mathrm{G}})}}\right)^{w} \tag{11}$$

The term including mass flux $G_{\mathrm{r}}$ in Eq. (11) is modified Froude number, where $d_{\mathrm{i}}$ is inner diameter of smooth tube, and in the case of micro-fin tubes, $d_{\mathrm{i}}$ is equivalent inner tube diameter. The exponents $p$, $q$, $r$, $w$ and the coefficient $A$ are determined from present and pervious data using the least squares method. Previous experimental data, mainly

Table 5: Multipliers and coefficient in Eq. (11)

| | *A* | *p* | *q* | *r* | *w* |
|---|---|---|---|---|---|
| Smooth | 0.158 | -0.75 | -0.42 | 0.35 | -0.40 |
| Mico-fin | 0.310 | -0.75 | -0.42 | 0.35 | -0.78 |

applied to this modification database, is listed in Table 4. The exponents *p*, *q* and *r* are assumed as common values in the case of smooth and micro-fin tubes. Table 5 lists those exponents and coefficients obtained from present and previous experimental data. In addition, comparison results from smooth tubes between present and previous data, void fraction and slip ratio against vapor quality, are shown in Fig. 8. Also, comparison results of micro-fin tubes are shown in the Fig. 9. The open symbols in Figs. 8 and 9 are void fractions. The closed symbols are slip ratios calculated from published void fraction data against vapor quality. From these comparison results, the present empirical correlation provides good agreement with experimental data.

## 4. CONCLUSIONS

The void fraction of $CO_2$ boiling flow in a horizontal micro-fin tube was investigated experimentally, and the results are compared with previous correlations proposed for smooth tube. Then, as a trial, Smith's model for smooth tube is modified to predict the slip ratio and the void fraction in both micro-fin and smooth tubes. The modified correlation agrees well with the present and previous experimental data for some refrigerants in smooth and micro-fin tubes. This correlation can also estimate the effects of mass flux.

## NOMENCLATURE

| | | |
|---|---|---|
| $x$ | vapor quality | ( - ) |
| $\xi$ | void fraction | ( - ) |
| $G_r$ | mass flux | ( kg m$^{-2}$ s$^{-1}$ ) |
| $P$ | pressure | ( Pa ) |
| $h$ | specific enthalpy | ( J kg$^{-1}$ ) |
| $m$ | mass | ( kg ) |
| $g$ | gravity acceleration | ( m s$^{-2}$ ) |
| $s$ | slip ratio | ( - ) |
| $\bar{u}$ | mean velocity | ( m s$^{-1}$ ) |
| $V$ | volume | ( m$^3$ ) |
| $d_h$ | equivalent inner diameter | ( m ) |
| $\mu$ | mass flux | ( Pa s ) |
| $\rho$ | density | ( kg m$^{-3}$ ) |

**Subscripts**

| | |
|---|---|
| G | vapor |
| L | liquid |
| void | sampling section |
| in | inlet |
| out | outlet |
| T | total |
| M | momentum |
| F | frictional |

## REFERENCES

Koyama, S., Lee, J.D.,Yonemoto, R., 2004, An investigation on void fraction of vapor-liquid two-phase flow for smooth and microfin tubes with R134a at adiabatic condition, *Int. J. Multiphase Flow*, vol. 30, p.291-310.

Yashar, D. A., Wilson, M.J., Chato, J. C., Kopke, H. R., Graham, D. M., Newell, T., 2001, An investigation of refrigerant void fraction in horizontal microfin tubes, *ASHRAE Trans.*, vol. 107, no.2, p.173-188.

Smith, S. L., 1971, Void fraction in two-phase flow, *Heat and Fluid Flow*.vol.1, no.1, p.22-39.

Butterworth, D, 1975, A comparison of some void fraction relationships for co-current gas-liquid flow, *Int. J. Multiphase Flow*, vol. 1 no.1, p.845-850.

Wojtan, L., Ursenbacher, T., Thome, J. R., 2004, Interfacial measurement in stratified type of flow, *Int. J. Multiphase Flow*, vol. 30, p.125-137.

Abdul-Razzak, A, Shoukri, M., Chang, J. S., 1995, Characteristics of refrigerant R 134a liquid-vapor two-phase flow in a horizontal pipe, *ASHRAE Trans.*, vol. 95, no.1, p.953-964.

Hashizume, K., 1983, Void fraction and flow regime of vapor-liquid two-phase flow in a horizontal smooth tube *JSME Trans.*, vol. 49, no. 473, p.189-196.(in Japanese)

Rohani, S. Z., Axelsson, E., 1970, Calculation of void volume fraction in the subcooled and quality boiling regions, *Int. J. Multiphase*, Vol. 13, p.383-393.

Bankoff, S. G., 1960, A variable density single-fluid model for two-phase flow with particular reference to steam-water flow, *Trans. ASME*, *J. Heat transfer*, Vol.82, p.265-272.

## ACKNOWLEDGEMENT

This investigation was partly supported by the Japan Refrigeration and Air conditioning Industry Association and the information of micro-fin tube was provided by Hitachi Cable, Ltd, which are gratefully acknowledged.